Classical trajectory studies of the unimolecular decomposition of the 2-chloroethyl radical

Thomas D. Sewell and Donald L. Thompson

Citation: The Journal of Chemical Physics **93**, 4077 (1990); doi: 10.1063/1.458740
View online: http://dx.doi.org/10.1063/1.458740
View Table of Contents: http://scitation.aip.org/content/aip/journal/jcp/93/6?ver=pdfcov
Published by the AIP Publishing

Classical trajectory studies of the unimolecular decomposition of the 2-chloroethyl radical

Thomas D. Sewell and Donald L. Thompson
Department of Chemistry, Oklahoma State University, Stillwater, Oklahoma 74078

(Received 23 March 1990; accepted 15 June 1990)

Classical trajectories have been employed in a study of the intramolecular dynamics and unimolecular decomposition of the 2-chloroethyl radical. A potential-energy surface was constructed by using the available experimental data and theoretical results. The following reaction channels were included in the study: $\cdot CH_2CH_2Cl \rightarrow CH_2 = CH_2 + \cdot Cl$, $\cdot CH_2CH_2Cl \rightarrow CH_2 = CHCl + \cdot H$. Mode-specific behavior was investigated by computing ensembles of trajectories for initial conditions (1) in which the normal-mode vibrations of the radical were assigned zero-point energies and a single C–H local stretch on the radical end of the system was excited, and (2) in which the normal modes were all excited so as to distribute the total energy uniformly throughout the radical. First-order rate coefficients were calculated both for the disappearance of the reactant and for the two chemically distinct reaction channels. The results do not indicate significant, if any, mode-specific effects. Energy transfer from and into local C–H stretching modes was studied. Relaxation of an initially excited C–H bond is observed to be irreversible and complete within about 0.6 ps.

I. INTRODUCTION

It is now well known that energy which is selectively deposited into a particular vibrational mode of a molecule (e.g., by direct laser pumping of high-frequency X–H overtones[1,2]) will, in many cases, transfer out of that mode along well-defined pathways.[3–36] This fact, along with a few tantalizing experimental indications of mode specificity, has prompted continuing interest in the possibility of inducing mode-specific behavior in chemical systems.[1,2,5,7–10,12–15,18,32,37–61]

There are a number of scenarios, linked by a common thread in that they are all inextricably tied to the nature of intramolecular vibrational relaxation, that would seemingly be conducive to mode-specific chemistry in polyatomic molecules. For example, if for a given reaction it were possible to preferentially excite modes that are intimately related to the reaction coordinate, then it might be possible to induce mode-specific reaction.[38,39] Another interesting situation arises in molecules containing two (or more) good local-mode X–H bonds in substantially different chemical environments. In such cases it may be possible to observe mode-specific effects due to qualitative differences in the IVR dynamics associated with the different bonds.[40–46] Also, intramolecular conversion processes (e.g., *cis–trans* isomerizations) provide interesting conditions for studying mode-specific behavior in unimolecular reactions.[2,7–10,18,47–53] The energy required for reaction, on the order of 10–30 kcal/mol, is much less than that required for bond fission. Indeed, unimolecular isomerization processes have provided some of the experimental evidence for mode-specific chemistry.[2,47,50,52] Heavy-atom blocking of IVR[33–36,59–61] has been suggested as a means of inducing mode-specific behavior, with both positive[59,61] and negative[60] results being reported. And, of course, van der Waals molecules are particularly well suited for observing nonstatistical behavior due to the weakness of the van der Waals bond.

Relaxation of excited C–H stretching modes occurs quite rapidly in many molecules, often on a time scale of a few tenths of a picosecond. Furthermore, with some reported exceptions,[12,17] the decay appears to be irreversible. If this rapid, irreversible loss of energy from the C–H bond occurs in such a way that the excess energy is quickly redistributed among most or all of the "bath modes" of the molecule then the chances of observing mode-specific behavior will be substantially decreased since it is usually necessary for a large fraction of the excitation energy to channel into the reaction coordinate. In spite of the speed with which energy decays from an excited C–H stretch, there is evidence that the relaxation usually involves fairly well-defined pathways.[16,17,19,21,22–31,45,46]

Since relaxation of C–H stretching modes occurs along specific pathways, why is mode specificity not more frequently observed for C–H overtone excitations? Part of the answer is that the upper limits to the energy that can be deposited in a molecule using single-photon C–H overtone excitations (ca. 50 kcal/mol) are usually close to the lower bounds of the energy required to surmount the barrier for bond-rupture reactions. Thus, if almost all of the excitation energy does not flow into the reaction-coordinate modes in the initial stages of energy redistribution, then the result is energy randomization rather than mode-selectively enhanced reaction. However, a recent study by Raff[54] indicates considerable mode specificity in the unimolecular reaction dynamics of 1,2-difluoroethane in spite of the fact that coarse-grain energy redistribution is complete on time scales shorter than the reaction lifetimes. This evidently provides an example of how relatively long-term retention of energy in groups of modes in a polyatomic molecule can, in at least some cases, lead to mode specificity. In molecules such as benzene, the initial relaxation occurs preferentially into the

 0021-9606/90/184077-17$03.00

bending modes but is then followed by efficient randomization among the active groups of normal modes.[23–26] Unless the group of normal modes is closely coupled to the reaction coordinate it is improbable that the energy retained in those modes will migrate into the reaction-coordinate modes and effect chemical reaction at a rate greater than some other initial excitation. When excitation of a methyl C–H overtone is used to cause a bond-rupture reaction not directly involving the methyl group, mode specificity is almost certain not to be observed because of the initial trapping of energy within the methyl group and the relatively slow transfer of energy from the methyl modes to the rest of the molecule.

In the present study we have investigated the influence of initial C–H stretch local-mode excitations on the decomposition of the 2-chloroethyl radical.[62–69] The study focuses on the simple bond-rupture reactions,

$$\cdot CH_2CH_2Cl \rightarrow CH_2 = CH_2 + \cdot Cl, \quad (R1)$$

$$\cdot CH_2CH_2Cl \rightarrow CH_2 = CHCl + \cdot H, \quad (R2)$$

with initial excitation of a C–H stretch on the radical end of $\cdot CH_2CH_2Cl$. The reaction channels, (R1) and (R2), have dissociation energies of approximately 20 and 35 kcal/mol, respectively.[67,68] These low dissociation energies are such that single-photon overtone excitation of a C–H stretching mode on the radical end of the reactant is capable of depositing energy in excess of that required for fission of the C–Cl and C–H bonds of the chloromethyl group.[70] In order to determine the effect of initial localization of the excitation energy, we calculated first-order rate coefficients for a uniform distribution of energy and compared them with the results for mode-selected initial conditions designed to simulate localized C–H overtone excitations. We have used a local-mode approximation[25] to compute the average energy content of each of the four C–H bonds in order to monitor the flow of energy as a function of time. The dependence of the calculated rate coefficients on the initial energy distribution is rationalized in terms of the energy transfer results.

II. METHOD OF CALCULATION

We have treated the three-dimensional dynamics of all the atoms in the 2-chloroethyl radical in a study of the C–Cl and C–H bond-rupture reactions, (R1) and (R2). We have formulated an approximate, anharmonic potential-energy surface that is in agreement with the available theoretical spectroscopic and thermochemical information about the radical[63,65,70] and reaction products.[71–79] Initial conditions simulating uniform and mode-selected distributions of energy were studied for five total energies in the range $70 \leqslant E \leqslant 118$ kcal/mol. The trajectories were calculated using methods that have been described previously.[80] Thus, we give only a brief description of the methods here.

A. Trajectory calculations

Ensembles of 200 trajectories were calculated for each set of initial conditions. Trajectories were calculated for total energies corresponding to zero-point energy plus excitation of a single C–H local mode to an overtone state ($v = 5$, 6, 9, 12, or 14). The trajectories were numerically integrated in a lab-fixed Cartesian coordinate system using a fourth-order Runge-Kutta-Gill routine with a fixed stepsize of 1.22×10^{-16} s. Integration accuracy was checked by varying the stepsize, monitoring energy conservation, and back integration. The maximum duration of a given trajectory was 20 ps for energies corresponding to excitation of the C–H local mode to $v = 5$, 10 ps for $v = 6$, 9, and 12, and 1.71 ps for $v = 14$.

We considered two qualitatively different types of initial conditions. In one case, all of the normal modes of the radical were assigned zero-point energies and a C–H local mode on the radical end of the system was excited to an overtone state. For the other type of initial conditions, a "uniform" distribution of energy was obtained by assigning each of the normal modes equal amounts of energy. The total angular momentum was zero in all of the calculations.

B. Analysis of the trajectories

Bond fission was considered to have occurred if the internuclear distance exceeded 2.25 Å or 3.42 Å for the C–H and C–Cl bonds, respectively. These criteria were chosen based on the Morse potentials, $V_M(r)$, that were used to represent the C–H and C–Cl stretches and are such that the ratio $V_M(r)/D_e = 0.95$, where D_e is the well-depth of the Morse potential. The time of dissociation was taken to be the time of the last inner turning point of the dissociating bond. Although all bond lengths were monitored throughout the trajectory calculations, only bonds of the chloromethyl moiety were observed to undergo dissociation.

First-order rate coefficients were calculated for the overall rate of decomposition for both types of initial conditions. The first-order rate coefficient, k, was obtained by fitting the trajectory lifetimes to

$$\ln(N_t/N_o) = -kt, \quad (1)$$

where N_t is the number of unreacted trajectories at time t and N_o is the total number of trajectories in the ensemble. Rate coefficients for the two dissociation channels, (R1) and (R2), were obtained by computing the ratio of the number of trajectories resulting in C–H bond fission, $N_{C\text{-}H}$, to the number of trajectories which ended in C–Cl bond rupture, $N_{C\text{-}Cl}$, and relating this ratio to the individual rates in the following manner:

$$k_{C\text{-}Cl}/k_{C\text{-}H} = N_{C\text{-}Cl}/N_{C\text{-}H} \quad (2)$$

$$k = k_{C\text{-}Cl} + k_{C\text{-}H}, \quad (3)$$

where $k_{C\text{-}Cl}$ is the rate coefficient for elimination of $\cdot Cl$ atoms and $k_{C\text{-}H}$ is the rate coefficient for the elimination of $\cdot H$ atoms.

Energy transfer within the 2-chloroethyl radical was monitored by computing the energy in the four C–H bonds using a local-mode approximation.[25] Averages of the C–H local-mode energies were computed for ensembles of trajectories corresponding to both types of initial conditions.

C. Potential-energy surface

The first step in the formulation of the potential-energy surface was to adjust the parameters of diagonal force-field potentials to achieve good agreement with theoretical nor-

mal-mode frequencies for the 2-chloroethyl radical,[67] and the experimental normal-mode frequencies for ethene[71] and chloroethene.[72] Having accomplished this, the next step was to develop reasonable switching functions that smoothly connect the potentials of the reactant and product species.

The potential-energy surfaces for the reactant and products were written as a sum of potential terms for the bond stretching, angle bending, and torsional motions. The stretches were represented by Morse functions,

$$V_M = D_e\{[1 - \exp(-\alpha(r - r_o))]\}^2, \quad (4)$$

where D_e is the dissociation energy, α is the curvature parameter, and r_o is the equilibrium bond length. Bending interactions were represented as harmonic oscillators,

$$V_b = 0.5f(\theta - \theta_o)^2, \quad (5)$$

where f is the force constant and θ_o is the equilibrium value of the angle. The torsional potentials were represented by six-term cosine series,

$$V_\tau = \sum_{i=0}^{5} a_i \cos(i\tau), \quad (6)$$

where τ is the dihedral angle. The a_i were adjusted to give the correct torsional frequency and barrier to internal rotation. As discussed below, the torsional potential was used only in the product molecules. There are six stretching terms, nine angle bending terms, four wag-angle bending terms, and six dihedral terms in the potential. No nondiagonal interaction terms were included in the potential-energy surface.

The numerical designations of the atoms and the definitions of the bonds and bond angles are given in Fig. 1. Equilibrium geometrical parameters for the 2-chloroethyl radical, ethene, and chloroethene are given in Table I. There have been several calculations of the equilibrium geometry of the 2-chloroethyl radical.[63,65–67,69] The structure used here is that reported by Schlegel and Sosa.[67] The equilibrium structure of ethene is taken from Raff[73] and the equilibrium geometry of chloroethene is based on the experimental structure reported by Kivelson and Wilson.[74] Experimentally, it has been determined that the geminal C–C–H bond angles of the chloroethene molecule have slightly different equilibrium values, as do the geminal C–H bonds.[74] Since these differences are small, we have taken the geminal C–C–H angles in chloroethene to be the same as in ethene and have used the average of the experimental values for the equilibrium geminal C–H bond length.

The force field for the 2-chloroethyl radical was obtained by adjusting the parameters to fit (unscaled) *ab initio* normal-mode frequencies.[67] Then, the bond-stretching parameters were scaled by 0.9 and angle-bending parameters by 0.8. These scale factors are comparable to those used by others,[51,81,82] and were found to give a fairly uniform (by about 10%) reduction in the values of all the normal-mode frequencies. Since the barrier to rotation about the C–C bond in the 2-chloroethyl radical has been reported to be 2–4 kcal/mol[63,66,67,69] the radical was treated as a free rotor.

Force-field parameters for the ethene and chloroethene molecules were adjusted such the calculated normal-mode frequencies are in good agreement with experimental values.[71,72] The barrier to internal rotation in ethene is between

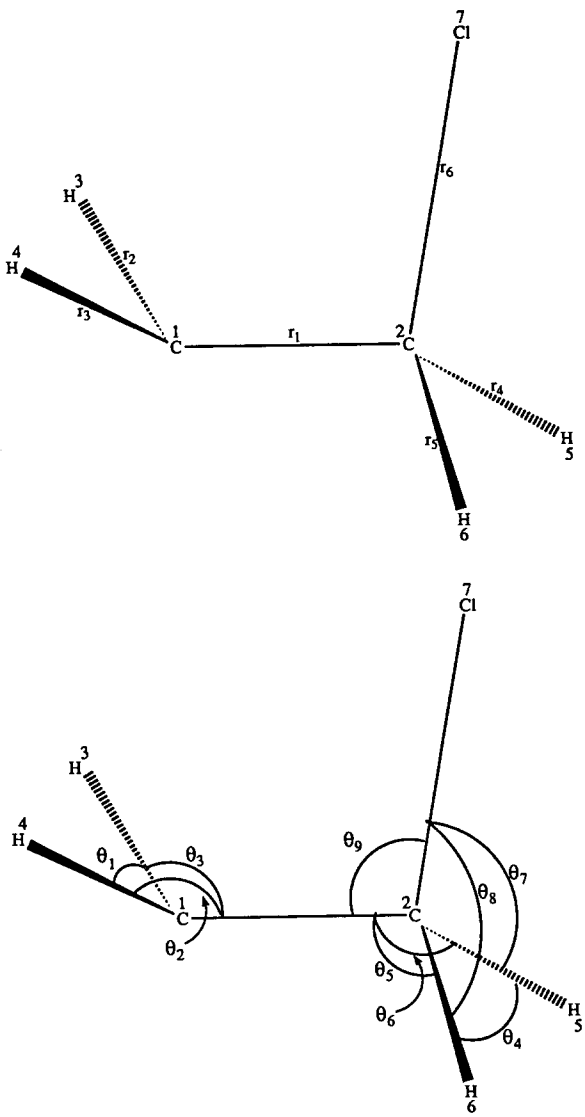

FIG. 1. (a) Definition of bonds and three atom bond angles in the 2-chloroethyl radical. (b) Numerical designation of atoms used to define wag angles and dihedral angles in the 2-chloroethyl radical.

60 and 65 kcal/mol.[75–79] We used the same value (63 kcal/mol) as used by Hase *et al.*[58] in their studies of the ethyl radical. The Fourier coefficients for the torsional potential of ethene and chloroethene were fit to give this barrier height. We assumed that the barrier to internal rotation for chloroethene is the same as for ethene. Force-field parameters for the 2-chloroethyl radical, ethene, and chloroethene are given in Table II. *Ab initio*, unscaled, and scaled normal-mode frequencies for the 2-chloroethyl radical are given in the first three columns of Table III, followed by the calculated and experimental normal-mode frequencies for ethene and chloroethene.

Switching functions were employed to smoothly connect the potential-energy surface and geometrical parameters for the 2-chloroethyl radical to those for the ethene and chloroethene molecules. The switching function employed is of the form[83]

$$S(r) = 1 - A\tanh[B(r - r^R)(r - C)^n], \quad (7)$$

TABLE I. Equilibrium geometrical parameters.[a]

Coordinate		Molecule		
Bond Number[b]	Bond Type	2-Chloroethyl Radical[c]	Ethene[d]	Chloroethene[e]
1	C–C	1.4508	1.353	1.332
2	C–H	1.0708	1.071	1.084[f]
3	C–H	1.0708	1.071	1.084[f]
4	C–H	1.0723	1.071	1.079
5	C–H	1.0723	1.071	···
6	C–Cl	1.9799	···	1.728
Angle Number	Angle Type			
1	H–C–H	118.2606	120.04	120.04
2	H–C–C	120.304	119.98	119.98
3	H–C–C	120.304	119.98	119.98
4	H–C–H	112.1544	120.04	···
5	C–C–H	115.3499	119.98	123.80
6	C–C–H	115.3499	119.98	···
7	H–C–Cl	101.5368	···	···
8	H–C–Cl	101.5368	···	113.90
9	C–C–Cl	108.8985	···	122.30
Wag Number	*X-Y-Z-W*[g]			
1	3-1-4-2	10.4432	0.0	0.0
2	5-2-6-1	39.8985	0.0	···
3	7-2-5-1	53.2494	···	···
4	7-2-6-1	− 53.2494	···	0.0
Dihedral Number	*W-X-Y-Z-A-B*[h]			
1	5-2-1-3-6-3	− 29.5191	0.0	···
2	6-2-1-4-5-2	29.5191	0.0	0.0
3	6-2-1-3-5-3	− 162.849	180.0	180.0
4	5-2-1-4-6-2	162.849	180.0	···
5	7-2-1-3-9-3	83.816	···	0.0
6	7-2-1-4-9-2	− 83.816	···	180.0

[a] Distances are in Å and angles are in degrees.
[b] See Fig. 1.
[c] Theoretical results from Schlegel and Sosa, Ref. 67.
[d] Values given by Raff, Ref. 73.
[e] Experimental results from Kivelson and Wilson, Ref. 74.
[f] Experimentally, the two C–H bond lengths were found to differ by 0.012 Å. The value used is the average of the two experimental values.
[g] Atom *W* is the wagging atom and atom *Y* is the anchor atom.
[h] *W*, *X*, *Y*, and *Z* are the atoms required to define the dihedral angle. *A* and *B* are bond angles.

where r is the bond length governing a particular switching function, r^R is the equilibrium bond length of the bond in the reactant molecule, and A is a dimensionless constant that depends upon both the parameter being attenuated and the bond on which the switching function depends. The parameters B, C, and n were adjusted to fix the rate at which $S(r)$ changes between the asymptotic limits. The values of the constants B, C, and n are 3.0×10^{-5} Å^{-17}, -0.08 Å, and 16, respectively, for switching functions defined in terms of C–H bonds, and 1.06×10^{-6} Å$^{-13.6}$, -3.0×10^{-3} Å, and 12.6, respectively, for the switching functions governed by the C–Cl bond. The purpose of the parameter A is to regulate the asymptotic limit of the switching function as the magnitude of the coordinate r changes and to simplify the simultaneous treatment of the three reaction channels. The instantaneous value of a parameter x ($x = D_e, \alpha, r_o, f, \gamma_o, \theta_o$, and a_i) is given by

$$x = x^P - (x^P - x^R)S(r), \tag{8}$$

where the superscripts R and P denote reactant and product, respectively.

For small and negative $r - r^R$, the switching functions controlled by bond r approach unity. As $r - r^R$ becomes large, the switching functions approach the asymptotic limit appropriate to the product being formed. Plots of the switching functions $S(r_{C\text{–}Cl})$ and $S(r_{C\text{–}H})$ are given in Fig. 2. The

TABLE II. Force-field parameters.

	2-Chloroethyl radical		Ethene		Chloroethene	
Morse parameters[a]						
Bond type	D_e (kcal/mol)	$\alpha(A^{-1})$	D_e (kcal/mol)	$\alpha(A^{-1})$	D_e (kcal/mol)	$\alpha(A^{-1})$
C–C	90.514	1.9111	148.835	1.905	148.835	1.85
·C–H	111.67	1.8304	···	···	···	···
C–H	35.0[b]	3.2175	116.4137	1.777	116.4137	1.7895
C–Cl	20.0[b]	2.6325	···	···	84.0[c]	1.7743
Harmonic force constants[d]						
Angle						
H–·C–H		54.1222	···	···		
H–·C–C		66.2133	···	···		
H–C–·C		92.1229	···	···	H–C–H	51.8191
	39.22	28.7884				
H–C–C		···	108.75	86.3652[e]		
				115.1536[f]		
H–C–Cl		93.2744	···	48.9403		
·C–C–Cl		161.215	···	···		
C–C–Cl		···	···	142.5025		
Wag Angle						
1		4.6061		15.9056	15.0	
2		0.0		15.9056	···	
3		0.0		···	···	
4		0.0		···	11.25	
Fourier coefficients[g,h]						
		a_0	a_2	a_4		
Ethene		6.7344	−7.9375	1.2031		
Chloroethene		6.8125	−7.9375	1.1250		

[a] Unless otherwise indicated, all D_e values were taken from Raff, Ref. 73.
[b] Values taken from Schlegel and Sosa, Ref. 67.
[c] R. T. Morrison and R. N. Boyd, *Organic Chemistry, 4th ed.* (Allyn and Bacon, Inc., Boston, 1983).
[d] Force constants are in kcal mol^{-1} rad^{-2} units.
[e] Angles involving ·H atoms on carbon atom #1 (see Fig. 1).
[f] Angle involving ·H atom on carbon atom #2 (see Fig. 1).
[g] kcal/mol.
[h] The 2-chloroethyl radical was treated as a free rotor.

labels "*A*" and "*B*" in Fig. 2 designate the switching functions defined in terms of the C–H and C–Cl bonds, respectively. In both cases the coefficient A [see Eq. (7)] is unity. Schlegel and Sosa[67] have reported calculations that indicate that when the C–Cl internuclear distance is 2.6 Å the molecular geometry is nearly the same as in the ethene molecule. For C–H bond distances greater than 2.0 Å the geometry closely resembles that of chloroethene. The rate of attenuation in our potential is somewhat slower than is implied by Schlegel and Sosa[67] for ·Cl elimination but is quite reasonable for C–H bond rupture. *Ab initio* molecular orbital calculations have been performed for the $H_2CCH_2F \rightarrow H_2CCHF + \cdot H$ system by Kato and Morokuma.[84] They examined the variations of some of the molecular parameters with extension of the C–H bond and found that the domain over which the individual parameters changed is relatively invariant. Thus, due to the lack of detailed knowledge concerning how individual potential and geometrical parameters vary in the 2-chloroethyl radical as a C–H or C–Cl bond undergoes dissociation, all parameters were attenuated using values for the constants B, C, and n that depended only on the nature (i.e., C–H or C–Cl) of the dissociating bond.

The overall attenuation of the potential is accomplished by defining three independent sets of switching functions, $\{S(r_4)\}$, $\{S(r_5)\}$, and $\{S(r_6)\}$. The bonds (r_4, r_5, and r_6) are the two C–H bonds and the C–Cl bond, respectively (see Fig. 1). The instantaneous value of some molecular param-

TABLE III. Theoretical, experimental, and calculated normal mode frequencies for the 2-chloroethyl radical, ethene, and chloroethene.

Frequency (cm^{-1})						
2-Chloroethyl radical			Ethene		Chloroethene	
Ab initio[a]	Unscaled[b]	Calculated[c]	Experimental[d]	Calculated	Experimental[e]	Calculated
309	–f	–f	826	824	395	397
316	321	287	943	881	620	493
415	459	412	949	1011	720	733
707	706	634	1073	1072	896	865
860	887	792	1220	1181	941	977
1113	1096	984	1342	1343	1030	1077
1124	1103	985	1444	1461	1279	1153
1323	1351	1208	1630	1656	1369	1376
1372	1368	1224	3021	2995	1608	1608
1602	1570	1403	3026	3015	3030	3018
1648	1682	1506	3103	3112	3086	3084
3319	3315	2992	3105	3129	3121	3136
3326	3328	3030				
3400	3421	3080				
3433	3440	3141				

[a] Schegel and Sosa, Ref. 67.
[b] Best fit to the *ab initio* frequencies.
[c] The bending force constants were scaled by 0.8 and the Morse curvature parameters were scaled by 0.9.
[d] Duncan, McKean, and Mallison, Ref. 71.
[e] Gullikson and Nielsen, Ref. 72.
[f] The 2-chloroethyl radical was treated as a free rotor.

eter x depends simultaneously on the values of r_4, r_5, and r_6:

$$x = x^P - (x^P - x^R)S(r_4)S(r_5)S(r_6). \tag{9}$$

When either of the three bonds that regulate switching functions undergo dissociation, the potential parameters (including those for the other two potentially reactive bonds) are attenuated to values appropriate for the product. If the differences between the reactant and product equilibrium bond lengths for the two remaining reaction–coordinate bonds are sufficiently small, then the attenuation of the potential is dominated by the set of switching functions defined in terms of the dissociating bond, with the two remaining sets of switching functions having little effect [i.e., as reaction occurs only one of the factors in the product in Eq. (9) deviates substantially from unity]. The differences between reactant and product equilibrium bond lengths for the relevant bonds are small enough that they can be neglected.

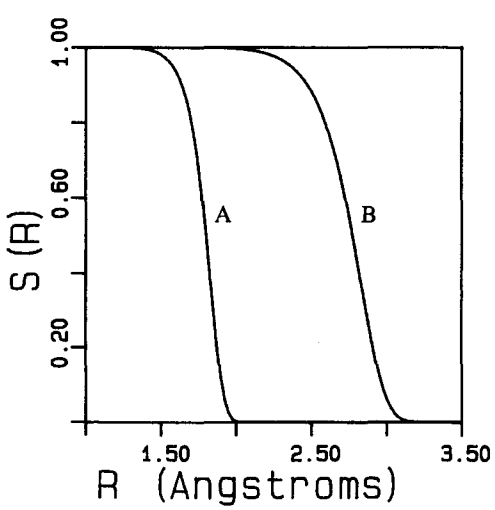

FIG. 2. Plot of the switching function used to attenuate molecular parameters as a function of the C–Cl bond length. The constant A is set to unity. Curve (A) is for the C–H bonds and curve (B) is for the C–Cl bond.

The values of the A parameters in Eq. (7) for each of the three dissociation channels were obtained in terms of the equilibrium geometries and force-field parameters of the 2-chloroethyl radical and the ethene molecule. Thus, the parameters x^R and x^P appearing in Eq. (9) were taken to be the equilibrium values for the 2-chloroethyl radical and ethene molecule, respectively. Hence, the constants A are unity for C–Cl dissociation (except in a small number of cases to be discussed below). The values of the constants A for the two C–H bond-rupture channels were obtained by solving for $S(r_{C\text{-}H})_\infty$ in the equation

$$z^P = x^P - (x^P - x^R)S(r_{C\text{-}H})_\infty. \tag{10}$$

Here, z^P is the value of a molecular parameter in chloroethene (corresponding to the parameters x^R and x^P in the 2-chloroethyl radical and ethene) and $S(r_{C\text{-}H})_\infty$ is the asymptotic limit of the switching function for the particular parameter under consideration. Using the explicit form of $S(r_{C\text{-}H})$ and Eq. (10) gives

$$1 - A\tanh[B(r - r^R)(r - B)^n] = (z^P - x^P)/(x^R - x^P). \tag{11}$$

As $r_{C\text{-}H}$ becomes large, $\tanh[B(r - r^R)(r - b)^n]$ approaches unity. Thus, the desired value for A is

$$A = 1 - (z^P - x^P)/(x^R - x^P). \tag{12}$$

TABLE IV. Switching function parameters.

Constants appearing in argument of tanh function [Eq. (7)]		
$B_{C\text{-}H} = 3.0\times10^{-5}$ Å^{-17}	$C_{C\text{-}H} = -0.08$ Å	$n_{C\text{-}H} = 16.0$
$B_{C\text{-}Cl} = 1.06\times10^{-6}$ Å$^{-13.6}$	$C_{C\text{-}Cl} = -0.003$ Å	$n_{C\text{-}Cl} = 12.6$

Reaction-channel and parameter-dependent constants, A (Eq. 7)[a]	Reaction channel	
Attenuated parameter	Bond four (C–H)	Bond five (C–H)
Eq. bond length		
r_1^0	1.214 723 926	1.214 723 926
r_2^0, r_3^0	66.0	66.0
r_4^0	0.0	− 5.153 846 154
r_5^0	− 5.153 846 154	0.0
r_6^0[b]	0.257 067 048	0.257 067 048
Angle number		
θ_4^0	− 2.809 4755	− 2.809 4755
θ_5^0	1.825 036 176	− 5.475 022 138
θ_6^0	− 5.475 022 138	1.825 036 176
θ_7^0	1.0	− 1.071 631 648
θ_8^0	− 1.071 631 648	1.0
θ_9^0	− 0.709 130 354	− 0.709 130 354
Wag number		
γ_2^0	− 0.408 570 727	− 0.408 570 727
γ_3^0	0.657 343 556	− 7.864 758 523
γ_4^0	− 7.864 758 523	0.657 343 556
Dissociation energy		
$D_{e,4}$	0.0	1.0
$D_{e,5}$	1.0	0.0
$D_{e,6}$[c]	2.133 333 3333	2.133 333 3333
Morse parameter		
α_1	10.016 393 44	10.016 393 44
α_2, α_3	0.840 650 894	0.840 650 894
α_4	0.0	0.991 294 828
α_5	0.991 294 828	0.0
α_6[d]	1.356 895 652	1.356 895 652
Force constant f_θ		
$f_{\theta,1}$	1.700 004 026	1.700 004 026
$f_{\theta,2}, f_{\theta,3}$	0.473 753 253	0.473 753 253
$f_{\theta,4}$	4.112 920 764	4.112 920 764
$f_{\theta,5}$	1.397 543 769	− 5.540 527 212
$f_{\theta,6}$	− 5.540 527 212	1.397 543 769
$f_{\theta,7}$	1.0	0.475 308 552
$f_{\theta,8}$	0.475 308 552	1.0
$f_{\theta,9}$	0.116 071 706	0.116 071 706
Force constant f_γ		
$f_{\gamma,1}$	0.919 854 861	0.919 854 861
$f_{\gamma,2}$	0.0	0.0
$f_{\gamma,3}$[e]	0.0	11.25
$f_{\gamma,4}$[e]	11.25	0.0
Dihedral angle		
τ_1, τ_4		
a_0	0.0	1.011 597 173
a_2	0.0	1.0
a_4	0.0	0.935 084 365
τ_2, τ_3		

TABLE IV (*continued*).

Constants appearing in argument of tanh function [Eq. (7)]

$B_{C\text{-}H} = 3.0\times10^{-5}$ Å^{-17}	$C_{C\text{-}H} = -0.08$ Å	$n_{C\text{-}H} = 16.0$
$B_{C\text{-}Cl} = 1.06\times10^{-6}$ Å$^{-13.6}$	$C_{C\text{-}Cl} = -0.003$ Å	$n_{C\text{-}Cl} = 12.6$

Reaction-channel and parameter-dependent constants, A (Eq. 7)[a]

	Reaction channel	
Attenuated parameter	Bond four (C–H)	Bond five (C–H)
a_0	1.011 597 173	0.0
a_2	1.0	0.0
a_4	0.935 084 365	0.0
τ_5, τ_6[f,g,h]		

[a] Any coefficient not explicitly shown is unity. In the case of footnotes b–h (below), $A_{C\text{-}Cl} = 0.0$.
[b] r_6^P is set to 1.0 Å and the switching function coefficients are adjusted so as to yield the correct equilibrium C–Cl bond lengths in all products.
[c] $D_{e_6}^P$ is set to 50.0 kcal/mol and the switching function coefficients are adjusted to yield the correct dissociation energies for all reaction products.
[d] α_6^P is set to 2.0 Å^{-1} and the switching function coefficients are adjusted to yield the correct curvature parameter for all reaction products.
[e] $f_{\gamma,6}^P$ is set to 1.0 and the switching function coefficients are adjusted to yield the correct wag angle harmonic force constants for γ_3 and γ_4 for all reaction products.
[f] a_0^P is set to 6.8125 kcal/mol and the switching function coefficients are adjusted to yield the correct Fourier coefficients for all reaction products.
[g] a_2^P is set to -7.9375 kcal/mol and the switching function coefficients are adjusted to yield the correct Fourier coefficients for all reaction products.
[h] a_4^P is set to 1.125 kcal/mol and the switching function coefficients are adjusted to yield the correct Fourier coefficients for all reaction products.

This is based on the requirement that the differences in the reactant and product equilibrium bond lengths be small for the bonds controlling the switching functions since there is really a product of three switching functions in Eq. (10). If the difference is sufficiently small, then the two remaining switching functions can be suppressed [as in Eq. (10)] since they will have values close to unity.

There is a complication in this formulation because the dissociating bond does not have an attenuating effect on itself and, as a consequence, some of the equilibrium parameters for the 2-chloroethyl radical and ethene are the same, rendering Eq. (10) inadequate. This difficulty was circumvented by "redefining" some of the x^P, which are the equilibrium parameters for the ethene molecule. The values of the affected A parameters for C–Cl dissociation are then determined in the same way as were those for C–H dissociation. The values of the A parameters for all three reaction channels are given in Table IV.

Figures 3 and 4 show the effect of C–Cl bond rupture on one of the torsional potentials and on the potential on one of the chloromethyl C–H bonds, respectively. The horizontal axis in Fig. 3 is the dihedral angle, the axis projected into the page is the C–Cl bond length, and the vertical axis is the torsional potential. The dihedral angle is a free rotor in the reactant (region A). As the C–Cl bond length increases the torsional potential varies with the value of the dihedral angle (region B). As the C–Cl bond length becomes sufficiently large the torsional potential assumes the form for $H_2C=CH_2 + \cdot Cl$ (region C).

Figure 4 is a contour plot demonstrating the attenuation of the potential of one of the chloromethyl C–H bonds as a function of the C–Cl bond length. The horizontal and vertical axes are the C–H and C–Cl bond lengths, respectively. The contours represent the potential energy of the C–H bond as a function of its extension and that of the C–Cl bond. Variation of the C–Cl bond length results in an attenuation of r_o, D_e, and α for the C–H bond. The figure illustrates that the equilibrium bond length changes by only a small amount (region A). However, the well depth and curvature of the C–H stretching potential show a marked dependence on $r_{C\text{-}Cl}$. For small $r_{C\text{-}Cl}$ the well depth is 35 kcal/mol, which is the contour extending out along the bottom right corner of the plot (region B). In the region where the switching functions are rapidly changing there is a corresponding change in the radial dependence of the C–H stretching potential (region C). The behavior for large $r_{C\text{-}H}$ clearly illustrates the attenuation of the C–H bond-stretching potential as the C–Cl bond length is increased. Finally, for large $r_{C\text{-}Cl}$ the Morse potential has become that for the ethene molecule (region D).

Graphical representations of the attenuation of individual molecular parameters as simultaneous functions of all three internal coordinates that govern attenuation of the potential-energy surface is not possible, but it is possible to illustrate the behavior of some of the parameters as two of the three coordinates are simultaneously varied. This is done in Figs. 5–7 for $D_{e_{C\text{-}C}}$, $\alpha_{C\text{-}C}$, and $r_{o_{C\text{-}C}}$, as simultaneous functions of the C–Cl bond length and one of the C–H bond

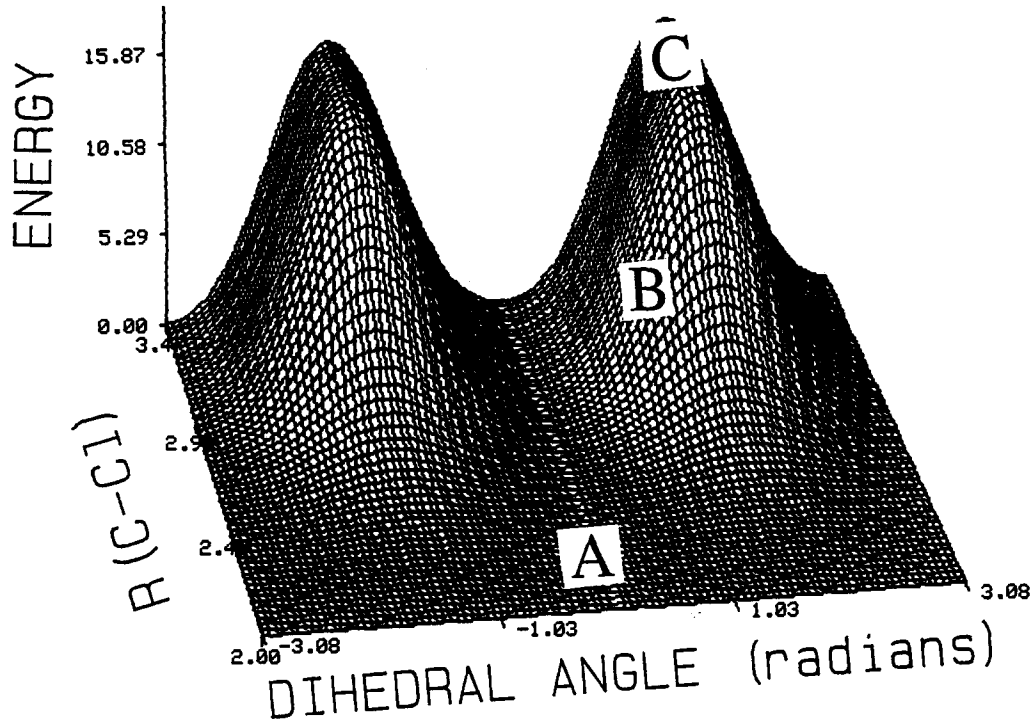

FIG. 3. Torsional potential (kcal/mol) for one of the dihedral angles as a function of the C–Cl bond length. (Å). All variables other than the dihedral angle and C–Cl bond length are frozen at their equilibrium values. Region *A* corresponds to the 2-chloroethyl radical. Region *B* corresponds to a C–Cl bond length substantially larger than its equilibrium value. Region *C* corresponds to $C_2H_4 + \cdot Cl$.

lengths. Regions *A*, *B*, and *C* in Figs. 5–7 correspond to the 2-chloroethyl radical, ethene, and chloroethene, respectively. Comparison of Figs. 5–7 with the values given in Tables I and II for the C–C bond-stretching parameters shows that the limiting behavior in the regions *A*, *B*, and *C* yield the correct asymptotic values for the parameters depicted. It is also clear from the figures that the domains over which the parameters are varying do not depend on the type of parameter being attenuated, but rather only on the type of bond dominating the attenuation of the potential. Finally, it was stated earlier that the entire switching formalism was defined in terms of the product obtained by the loss of a chlo-

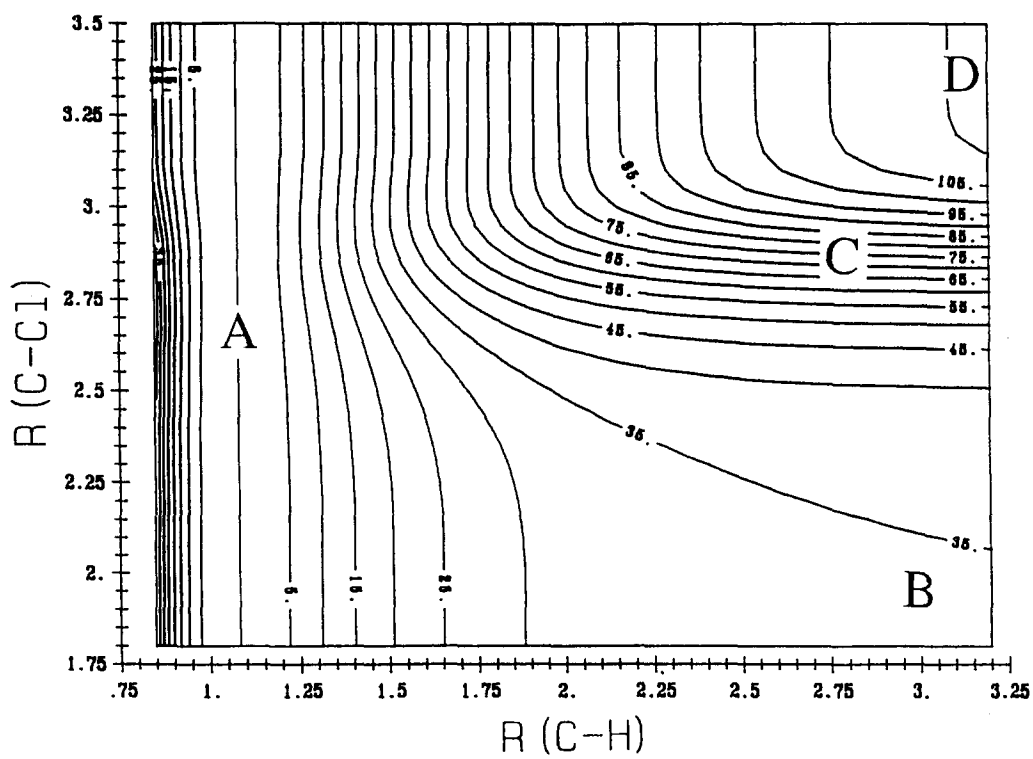

FIG. 4. Contour plot illustrating the effect of ·Cl elimination on the potential-energy function for one of the reactive C–H bonds. The contour denoted by "*A*" shows the location of the minimum potential energy in the C–H bond as the molecule decomposes through the C–Cl channel. Region *B* corresponds to the energy required to rupture a C–H bond in the reactant molecule. Region *C* shows the potential in transition from that of the reactant species to that of ethene. Region *D* corresponds to the C–H stretching potential for loss of ·Cl. Distances are in Å and energies are in kcal/mol.

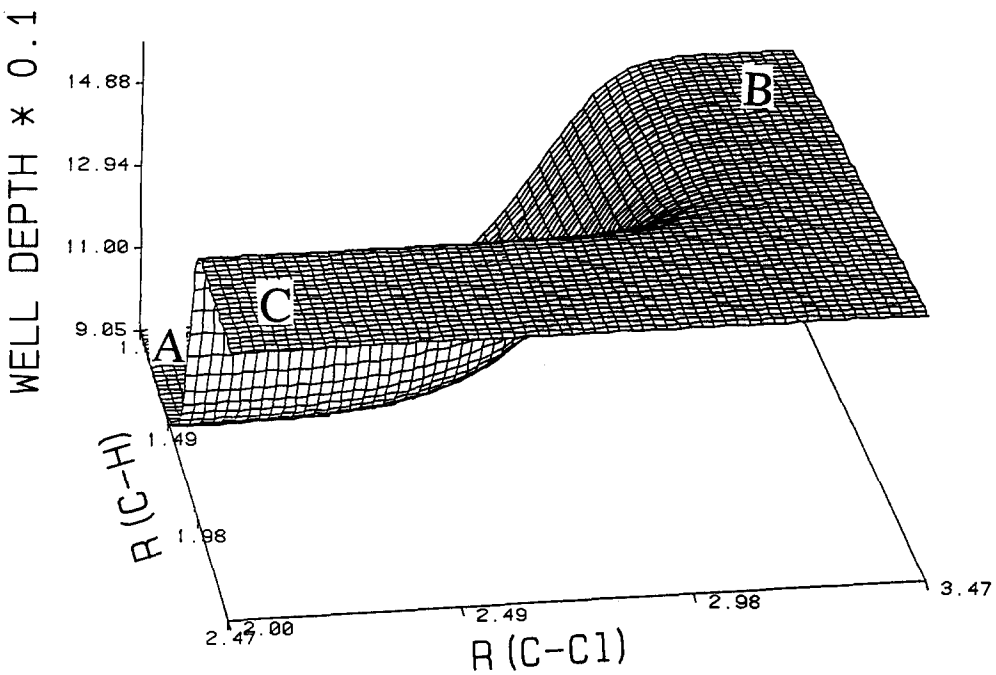

FIG. 5. Plot showing the behavior of the dissociation energy for the C–C bond as a simultaneous function of the C–Cl and C–H bond length in the 2-chloroethyl radical. The actual energies are ten times those shown in the figure. Region *A* corresponds to the equilibrium well depth of the C–C bond in the reactant. Regions *B* and *C* correspond to the equilibrium well depths in the ethene and chloroethene molecules, respectively. Distances are in Å and energies are in kcal/mol.

rine atom. This is evident in Figs. 5–7 which show that, in the unlikely event that the C–Cl bond and one (or more) of the two C–H bonds simultaneously undergo dissociation, the resulting value of a given parameter will take on the value appropriate to ethene. This does not pose a problem for the energies we considered.

Figure 8 is a plot of the minimum potential energy of the 2-chloroethyl radical system for the elimination of a ·Cl atom. The curve was generated by numerically searching the configuration space of the 2-chloroethyl radical and recording the minimum potential energy obtained for a given C–Cl extension. Circles in Fig. 8 indicate the fixed C–Cl bond lengths for which a search was performed. The circles are connected by straight lines. The relative energy difference between the reactant and the $C_2H_4 + \cdot Cl$ product is 20 kcal/mol, as dictated by theoretical calculations.[67,68] Examina-

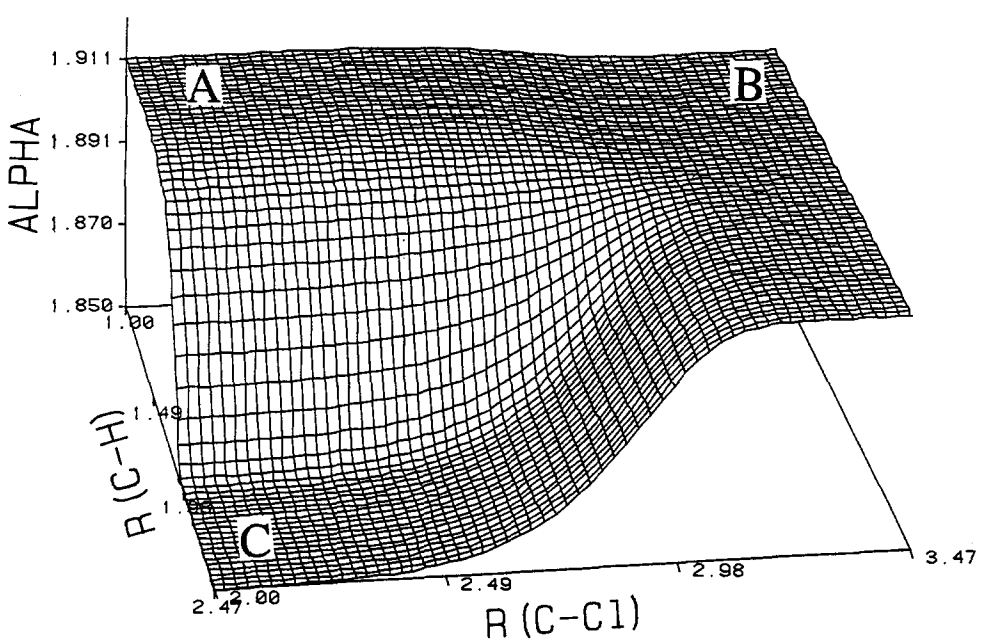

FIG. 6. Same as Fig. 5, except for the behavior of the C–C bond exponential curvature in the Morse function. The curvature parameter is given in $Å^{-1}$.

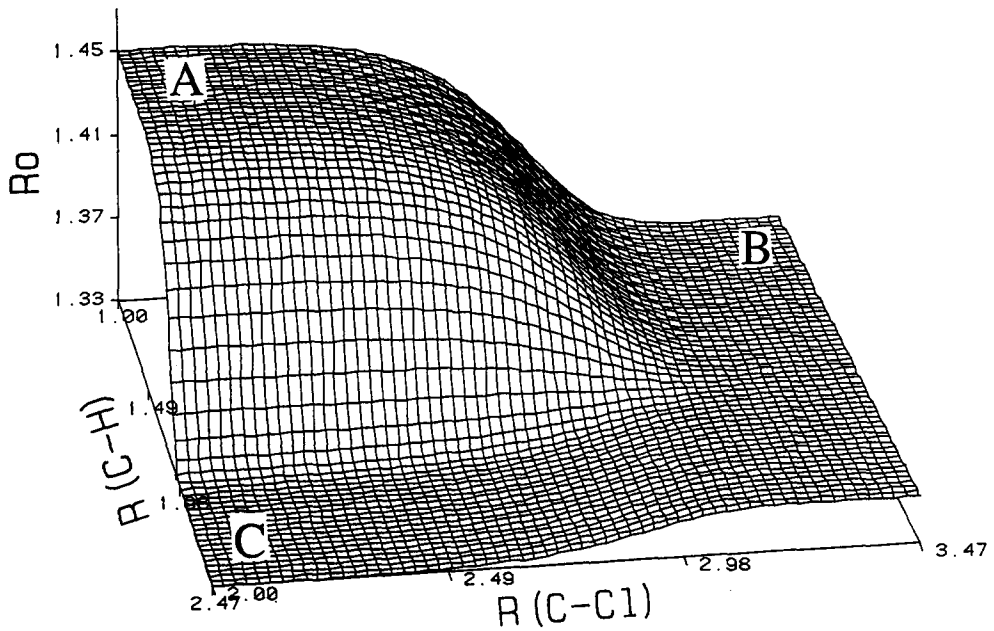

FIG. 7. Same as Fig. 5, except for the behavior of the equilibrium C–C bond length (in units of Å).

tion of the minimum-energy molecular configurations generated in the searches did not indicate any discontinuities in the internal coordinates along the minimum-energy profile.

III. RESULTS AND DISCUSSION

We have used classical trajectory methods to calculate first-order rate coefficients for the two bond-rupture reactions (R1) and (R2) of the 2-chloroethyl radical for two different types of initial conditions, one corresponding to local excitation of a C–H bond and the other to a uniform distribution of energy among the normal modes of the reactant. The impetus for the study was to investigate the possibility of mode-specific reaction.

The computed first-order rate coefficients are summarized in Table V, according to both the type of excitation scheme used and the total system energy. The quantum number v in the first column of Table V indicates the level of excitation of the C-H bond for initial conditions in which all of the energy in excess of the zero-point level is initially localized in a single C–H local mode. The energy in the next-to-last column of Table V is the total energy of the 2-chloroethyl radical (including the zero-point energy). The maximum duration of a trajectory t_{max}, at a given energy, is given in the last column of Table V. The overall first-order rate coefficients k are calculated from Eq. (1). The rate coefficients for ·H and ·Cl elimination, k_{C-H} and k_{C-Cl}, respectively, are calculated using the overall rate coefficient, k, and Eqs. (2) and (3). The numbers of trajectories leading to elimination of ·H and ·Cl in a given ensemble of trajectories are given by N_{C-H} and N_{C-Cl}, respectively. Thus, the total number of reactive trajectories in any particular ensemble is $N_{C-H} + N_{C-Cl}$. A total of 200 trajectories were computed for each set of initial conditions.

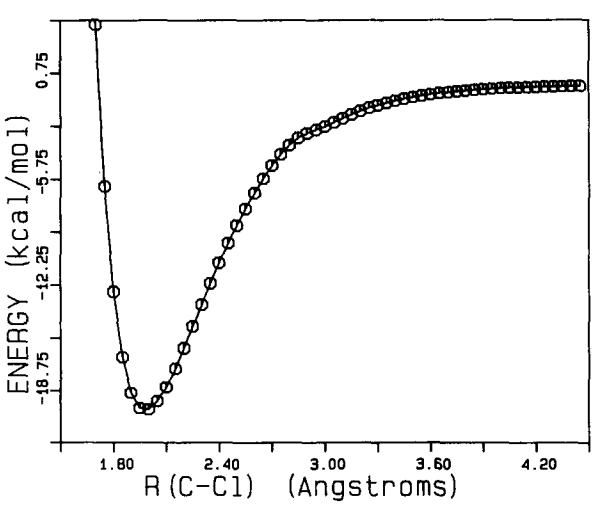

FIG. 8. Plot of the potential energy of the 2-chloroethyl radical system as the C–Cl bond length is incrementally increased and the remaining internal coordinates are relaxed.

We computed ensembles of trajectories for energies corresponding to a C–H local-mode excitation to the $v = 5$ level (total energy of 69.8 kcal/mol). This energy approaches those attainable in the laboratory. Trajectories at this energy were integrated for up to 20 ps. Fifty-five percent of the trajectories underwent reaction within this time cutoff for both types of initial conditions. For the local-mode excitation, 10 trajectories led to ·H elimination and 100 led to loss of ·Cl. Rupture of C–H and C–Cl bonds occurred 12 and 98 times, respectively, for the uniform excitation. The calculated rate coefficients at this energy do not indicate a significant dependence on the type of excitation. Local-mode excitation led to an overall rate coefficient of 0.041 ps^{-1} while uniform excitation resulted in a rate coefficient of 0.040 ps^{-1}. The branching ratios for the two excitation schemes are similarly in close agreement. The rate coefficient for C–Cl bond rupture is 0.037 ps^{-1} for local-mode excitation and 0.036 ps^{-1}

TABLE V. Rate coefficients.[a]

	Local-mode excitation					Uniform excitation						
v[b]	k	k_{C-H}	(N_{C-H})	k_{C-Cl}	(N_{C-Cl})	k	k_{C-H}	(N_{C-H})	k_{C-Cl}	(N_{C-Cl})	Energy[c]	t_{max}[d]
5	0.041	0.004	(10)	0.037	(100)	0.040	0.004	(12)	0.036	(98)	69.8	20.0
6	0.058	0.006	(8)	0.053	(77)	0.073	0.007	(9)	0.066	(84)	76.5	10.0
9	0.193	0.057	(49)	0.138	(117)	0.219	0.070	(54)	0.150	(116)	94.6	10.0
12	0.379	0.159	(82)	0.221	(114)	0.372	0.156	(82)	0.216	(114)	109.0	10.0
14	0.486	0.203	(40)	0.284	(56)	0.526	0.240	(52)	0.286	(62)	117.8	1.7

[a] Rate coefficient units are ps^{-1}.
[b] C–H local-mode quantum number.
[c] Total energy in kcal/mol.
[d] Maximum trajectory integration time in ps.

for uniform excitation. The rate coefficient for C–H bond rupture is 0.004 ps^{-1} for both excitation schemes. The first-order decay curves for energies corresponding to $v = 5$ local-mode excitation (69.8 kcal/mol) are given in Fig. 9. Asterisks and open circles in Fig. 9 represent calculated lifetimes for uniform and local-mode excitations, respectively. The solid lines are least-squares fits to the data. There is a period of about 0.75 ps during which the only observed lifetimes arise from the initially uniform distribution of energy. This is because of the time required (following local-mode excitation of a C–H bond on the $\cdot CH_2$ group) for energy to transfer from the excited C–H bond of the $\cdot CH_2$ group to the chloromethyl group. For initial conditions in which the energy is evenly distributed over the normal modes more energy is located in the chloromethyl moiety than in the $\cdot CH_2$ group and the reactant can dissociate almost immediately. The time lag decreases as the energy in the 2-chloroethyl radical is increased.

The first-order rate coefficients for energies corresponding to zero-point energy plus local-mode excitation of a C–H bond to the $v = 6$ level (total energy of 76.5 kcal/mol) follow the behavior of those for $v = 5$ (Table V). The time cutoff for trajectories computed at this energy was 10 ps. For the local-mode excitation at this energy a total of 85 trajectories underwent reaction within 10 ps. Eight of these led to C–H rupture with the remaining 77 resulting in fission of the C–Cl bond. Uniform excitation at the same energy led to 93 reactive events, 9 of which were C–H dissociations. There were 84 C–Cl bond ruptures. Thus, the major difference between the two ensembles at this energy is the increase in

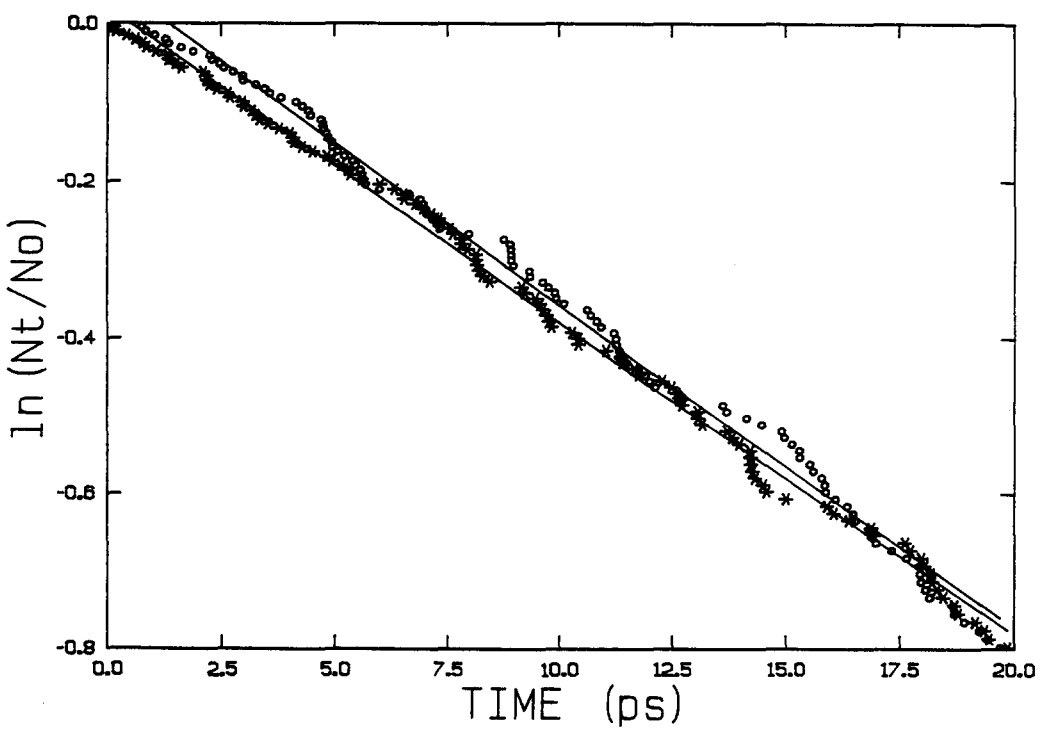

FIG. 9. First-order decay curve for the overall decomposition of the 2-chloroethyl radical at an energy corresponding to zero-point energy plus excitation of a single C–H local mode to the $v = 5$ state. (*) denotes initial conditions corresponding to uniform distribution of energy over the normal modes of the molecule. (O) denotes initial conditions corresponding to excitation of a single C–H stretch. The straight lines are least squares fits to the data.

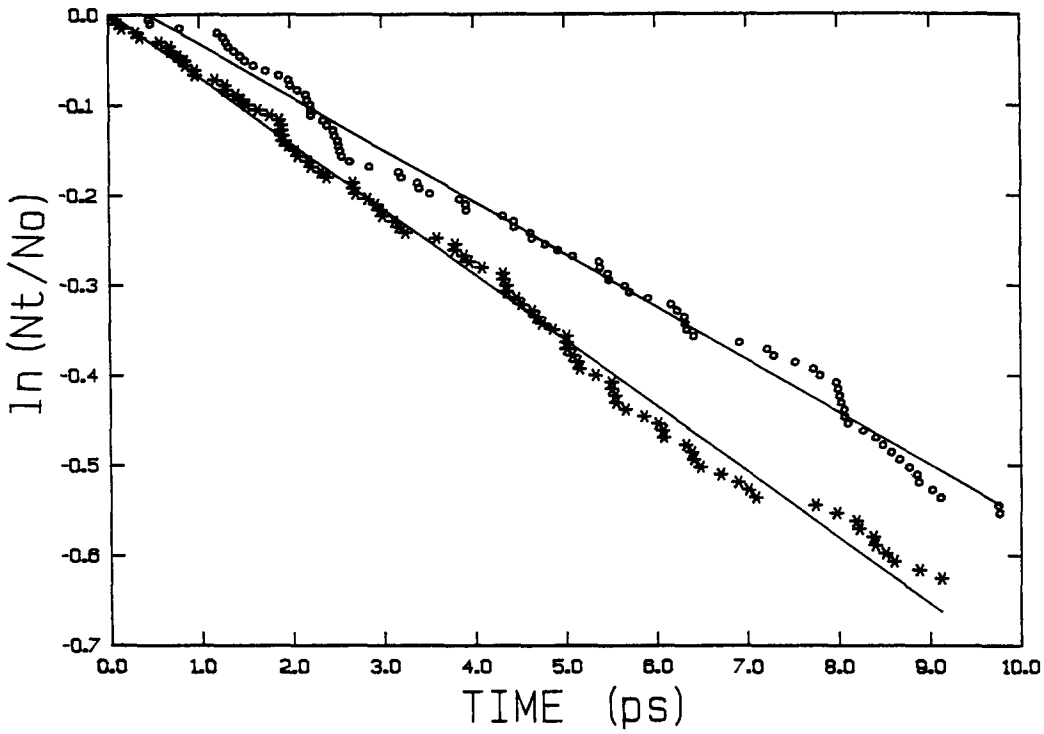

FIG. 10. Same as Fig. 9, except for a $v = 6$ local-mode excitation.

the number of C–Cl dissociations for an initially uniform distribution of the energy, a result we tentatively attribute to the small number of trajectories calculated. The overall first-order rate coefficient for C–H local-mode excitation to $v = 6$ is 0.058 ps^{-1}. Uniform excitation led to a computed rate coefficient 1.26 times as large, with a value of 0.073 ps^{-1}. The major difference in the rate coefficients appears in the C–Cl channel. The factor of 1.26 in the rates obtained for the two excitation schemes is the largest obtained in our study. Local-mode excitation led to a rate coefficient for C–Cl bond rupture of 0.053 ps^{-1} while the uniform distribution of energy led to a rate coefficient of 0.066 ps^{-1}. The first-order rates for C–H fission at this energy are nearly equal, with the local-mode and uniform excitation leading to rate coefficients of 0.006 ps^{-1} and 0.007 ps^{-1}, respectively. The decay curves for trajectories calculated at this energy are given in Fig. 10. Once again there is a time lag between the first lifetime for uniform and local-mode excitations, although in this case the delay (0.44 ps) is somewhat smaller than before (0.75 ps in Fig. 9). The difference between the slopes in Fig. 10 is small and, we think, is a consequence of the small number of reactive trajectories. There are gaps in the decay curve for the local-mode excitation, results that are probably a consequence of the small ensemble size. Based on the relatively small discrepancy between the computed values of the rate coefficients and the large uncertainty in the rate coefficients obtained from so few lifetimes, we do not believe that mode-specific effects are important at this energy.

The behavior of the first-order rate coefficients computed for higher energies is qualitatively similar to that for lower energies. The zero-point energy plus that due to excitation of a C–H local mode to $v = 9$ gives a total energy of 94.6 kcal/mol. At this energy 166 of 200 trajectories reacted within 10 ps following local-mode excitation. Of these, 49 were C–H dissociations and 117 were C–Cl ruptures. Uniform distribution of the same total energy resulted in 170 reactive events, with 54 and 116 C–H and C–Cl fissions, respectively. In contrast to the previous case for which the main difference in reactivity appeared to be an increase in the number of C–Cl bond ruptures for the uniform distribution of the energy, here the reverse is true with local-mode excitation giving rise to one more C–Cl bond fission than uniform distribution of energy, but with the latter leading to five more C–H ruptures. The overall first-order rate for local-mode excitation at this energy is 0.193 ps^{-1} and that for uniform distribution of the energy is 0.219 ps^{-1}, the latter being larger by a factor of 1.13. The rate coefficients for C–H bond-rupture are 0.057 ps^{-1} and 0.070 ps^{-1} for local-mode and uniform excitation, respectively. Rate coefficients for C–Cl bond fission are 0.138 ps^{-1} and 0.150 ps^{-1} for local-mode and uniform excitation, respectively. Once again, the differences in the computed rate coefficients are small and are probably attributable to statistical error due to the small ensemble sizes.

Zero-point energy plus excitation of the C–H local mode to $v = 12$ results in a total energy of 109.6 kcal/mol. Of the 200 trajectories calculated for local-mode excitations at this energy, 196 underwent reaction within the 10 ps time cutoff. The same number reacted following uniform distribution of the same total energy. Moreover, the number of C–H and C–Cl bond ruptures were identical in both ensembles, with 82 C–H and 114 C–Cl dissociations, respectively, in both ensembles. The overall first-order rate coefficients are almost identical, with values of 0.379 ps^{-1} and 0.372 ps^{-1} for local-mode and uniform excitation, respectively. The rate coefficients for ·H and ·Cl elimination are 0.159 ps^{-1} and 0.221 ps^{-1}, respectively, following local-mode excitation

and 0.156 ps^{-1} and 0.216 ps^{-1}, respectively, following uniform distribution of the energy among the normal modes of the reactant.

The largest energy for which we calculated trajectories is 117.8 kcal/mol, which corresponds to zero-point energy plus excitation of the C–H local mode to $v = 14$. The maximum duration of trajectories at this energy was 1.7 ps. During this time 96 of 200 trajectories resulted in reaction following local-mode excitation, with 40 and 56 trajectories leading to C–H and C–Cl bond rupture, respectively. For a uniform distribution of the same total energy 114 trajectories reacted, with 52 and 62 trajectories reacting through the C–H and C–Cl channels, respectively. The overall first-order rate obtained for uniform distribution of the energy is 1.08 times that for local-mode excitation, the prior having a value of 0.526 ps^{-1} and the latter a value of 0.486 ps^{-1}. The greatest difference in the rate coefficients is in the C–H channel, with local-mode excitation giving a value of 0.203 ps^{-1} and uniform distribution of the energy a value of 0.240 ps^{-1}. The computed rate coefficients for the C–Cl channel are in near agreement, with values of 0.284 ps^{-1} and 0.286 ps^{-1} for the local-mode and uniform excitations, respectively.

The overall first-order rate coefficients increase exponentially with the total energy, and the rate coefficients are well described using the classical RRK formula,[85]

$$k(E) = A(1 - E_o/E)^{s-1}, \tag{13}$$

where $k(E)$ is the overall first-order rate coefficient at a given energy E, A is the frequency factor, E_o is the minimum energy required for reaction, and s is the number of degrees of freedom in the system. For a collection of classical oscillators that is well described statistically, a plot of $\ln k(E)$ vs $\ln(1 - E_o/E)$ yields a straight line having an intercept of $\ln(A)$ and a slope of $s - 1$. The normal implementation of Eq. (13) is to use the rate coefficients $k(E)$ and the critical energy E_o to obtain an estimate of the number "effective degrees of freedom" in the molecule, s.

Application of Eq. (13) to the data in Table V yields good least-squares fits ($R^2 = 0.98$ or better). The results of this fitting procedure for the 2-chloroethyl radical are given in Table VI. Results for both the overall first-order rate coefficients and the C–H/C–Cl branching ratios and for both types of excitation schemes are given. The value of the critical energy E_o used to fit the overall rate coefficients is the weighted average of the C–H and C–Cl dissociation energies. Since there two C–H bond-rupture channels and only one for C–Cl bond rupture, the value of E_o is $(2D_{e,C-H} + D_{e,C-Cl})/3.0 = 30.0$ kcal/mol. The dissociation energies of the C–H and C–Cl bonds (35.0 and 20.0 kcal/mol, respectively) were used for the calculations involving the branching ratios. Comparison of the results presented in Table VI for the two excitation schemes suggests that the initial distribution of energy in the 2-chloroethyl radical does not play an important role in the reaction dynamics. The value of s for the overall rate-coefficient data is calculated to be 10.5 for both the localized and uniform distributions of energy. The results obtained for the branching ratios are similarly in good agreement. The calculated values of s for the C–H channel are 13.6 and 13.3 for the local-mode and uniform excitation schemes, respectively. The C–Cl channel s values are 14.5 and 14.2 for the local-mode and uniform excitations, respectively. The theoretical value is $s = 3N - 6$ for a molecule consisting of N atoms. However, for many polyatomic molecules the effective number of degrees of freedom calculated by fitting Eq. (13) to experimental data is considerably less than the theoretical value. In the case of the 2-chloroethyl radical, the effective number of degrees of freedom for reactions (R1) and (R2) is close to the theoretical value (within about 3%–11% of the theoretical prediction), a result that may be a consequence of the extensive potential-energy coupling due to the switching functions. While the close agreement between the RRK fits for the local-mode and uniform excitations does not prove that mode-specific effects are unimportant in the 2-chloroethyl radical, they do lend further support to the conclusions presented above in the discussion of the individual rate coefficients. Moreover, the quality of the fit of the results in Table V to Eq. (14) suggests that the energy dependence of the first-order rate coefficients for the 2-chloroethyl radical is described by RRK theory, which is based on statistical assumptions.

TABLE VI. Calculated RRK s parameter

Local-mode excitation			Uniform excitation		
k_{tot}	k_{C-H}	k_{C-Cl}	k_{tot}	k_{C-H}	k_{C-Cl}
10.5	13.6	14.5	10.5	13.3	14.2

Reinhardt and Duneczky[32] have reported the results of calculations performed on a model of the 2-chloroethyl radical. They compared lifetime distributions for C–Cl fission during the first picosecond following excitation of C–H bonds on different ends of the reactant. C–H fission was not considered in their study since they treated the four C–H bonds as being "almost isoenergetic". They found that, for excitations of one of the C–H bonds to $v = 5$ or $v = 6$, there is a propensity for "prompt" reaction to occur when one of the chloromethyl group C–H bonds was excited, suggesting that short-time localization of energy does occur. The effect becomes more pronounced with increasing energy, with the $v = 6$ excitation giving about twice as many "prompt" reactions as the $v = 5$ excitation. This is in accord with the results of a number of calculations dealing with IVR following methyl C–H excitation, in which energy appears to be temporarily trapped in the methyl-group modes, leaking "slowly" to the remainder of the molecule.[17,28,29,45,49] Also, their observations are in accord with those reported here insofar as we see "prompt" dissociation following uniform initial distributions of energy (relative to highly localized excitations of the $\cdot CH_2$ group). There are more degrees of freedom associated with the chloromethyl moiety than with the $\cdot CH_2$ group and, thus, uniformly distributing energy over the normal modes of the 2-chloroethyl radical places more energy in the chloromethyl group than in the $\cdot CH_2$ group, as pointed out above.

The results for the computed first-order rate coefficients

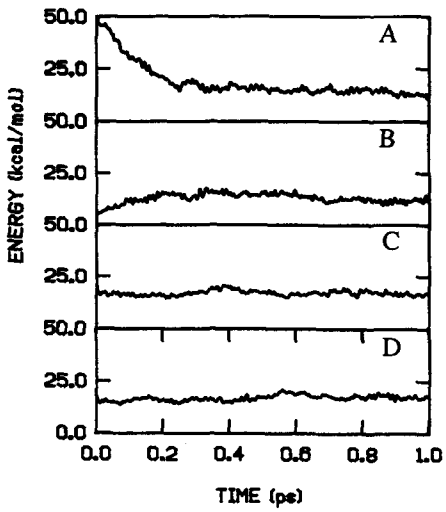

FIG. 11. Average energy of the C–H local modes of the $\cdot CH_2$ group as a function of time. (a) C–H stretch locally excited to the $v = 6$ state. (b) Same as (a), except for the initially unexcited C–H bond. (c) and (d) Same as (a) and (b), except for a uniform distribution of 117.8 kcal/mol of energy.

indicate that the initial distribution of energy has little or no effect on the rate of reaction in the 2-chloroethyl radical. One explanation for this observation is that the time scale for energy randomization is significantly shorter than that for chemical reaction. We have monitored the energy redistribution in the 2-chloroethyl radical as a function of time by using a local-mode approximation[25] to compute the energies of the four C–H bonds. Ensembles of 25 trajectories were followed for 1.0 ps and the average energies in the C–H local-modes were obtained for zero-point energy plus a C–H overtone excitations to $v = 3$, 6, 8, 10, or 12. An ensemble of 100 trajectories was computed for both types of initial conditions and the C–H local-mode energies were averaged for an energy corresponding to zero-point energy plus a $v = 14$ overtone excitation. In all cases the averaging was appropriately weighted if a trajectory underwent dissociation before the time cutoff. Results representative of these calculations are given in Fig. 11. In Fig. 11 the top curve, (A), is the average local-mode energy in an initially excited C–H bond of the $\cdot CH_2$ group. The C–H bond is excited to the $v = 6$ level. The second curve, (B), is the average local-mode energy in the initially unexcited C–H bond of the $\cdot CH_2$ group. Curves (C) and (D) correspond to the same bonds as in (A) and (B) for the case of a uniform distribution of 117.8 kcal/mol of energy (equivalent to zero-point energy plus excitation of a C–H bond to $v = 14$). The energy-transfer results for excitation of the C–H local mode to $v = 3$, 8, 10, 12 and 14 are qualitatively very similar to those shown in Fig. 11 and are therefore not presented here.

For this wide range of energies the relaxation of the initially excited C–H local mode is fast and irreversible. There is a rapid, short-time transfer of energy lasting ~ 0.15 to 0.20 ps followed by a slower relaxation. The energy in the initially unexcited C–H bond of the $\cdot CH_2$ group increases more rapidly than do the energies of the chloromethyl C–H bonds, both of which increase in energy at approximately the same rate. Roughly 50% of the energy in the excited C–H bond (curve A in Fig. 11) has been lost within about 0.15 ps. The sum of the C–H local-mode energies comprises roughly one-half to three-quarters of the total energy in the 2-chloroethyl radical after equilibration of energy among the C–H local modes. In all cases the energy has become evenly distributed among the C–H local modes within about 0.6 ps. Curves (C) and (D) demonstrate the expected result that, when the trajectories are begun with a uniform distribution of energy, the energy remains evenly distributed.

The mean lifetime (k^{-1}) of the set of initial conditions yielding the largest rate coefficient (uniform distribution of 117.8 kcal/mol of energy among the normal modes) is calculated to be 1.9 ps. Thus, based on the energy transfer results for the C–H local modes, the time required for the "average" trajectory to react under these conditions is roughly 3.3 times larger than that needed for energy randomization. The mean lifetimes for the $v = 5$ excitations are much larger, having values of about 24 ps. In this case the ratio of the "average" time required for reaction to the time needed for energy randomization increases from 3.3 to 40. Energy redistribution is complete long before most trajectories react and, as a consequence, the calculated first-order rate coefficients obtained for initial conditions in which all of the energy in excess of the zero-point level is localized in a single C–H bond are essentially the same as those obtained for initial conditions in which the same total energy is distributed uniformly over the normal modes of the reactant. Mode-specific effects due to C–H local-mode excitation do not appear to be important in the unimolecular decomposition of the 2-chloroethyl radical.

IV. SUMMARY

We have performed classical trajectory calculations to investigate the possibility of mode-specific unimolecular dissociation in the 2-chloroethyl radical. Ensembles of trajectories were computed for five different total energies and two different types of initial conditions. Rate coefficients for initial conditions corresponding to C–H local-mode excitations were compared to rate coefficients for the same total energy uniformly distributed over the reactant. These results indicate little or no difference in the overall rate coefficients for the two types of initial conditions, and the branching ratios for the $\cdot Cl$ and $\cdot H$ elimination reactions are approximately the same for both types of initial conditions. These results suggest that there is no mode specificity for C–H local-mode excitations.

The observed lack of mode-specific behavior is seemingly reconcilable with the rates of intramolecular energy transfer obtained using a local-mode approximation. The time required for relaxation of an initially excited C–H bond is roughly 32% of that required for the average dissociative trajectory to react under conditions yielding the shortest average lifetime. Assuming that C–H local mode energies are a valid measure of energy content within the radical, redistribution of energy is complete before most trajectories undergo dissociation. This result is in accord with most of the theoretical and experimental evidence to date for various systems.

Both types of excitation schemes employed in this study lead to linear RRK plots, suggesting that the 2-chloroethyl radical behaves statistically with respect to the energy dependence of the rate coefficients. Calculated values of the RRK s parameter do not depend strongly on the initial distribution of energy.

ACKNOWLEDGMENTS

This work was partially supported by the U.S. Army Research Office. Some of the calculations were carried out on the Cray X-MP/48 at the National Center for Computing Applications at Urbana-Champaign. TDS would like to thank Carlos Sosa, James Myers, and Matthew Cote for useful discussions during the course of this work.

[1] F. F. Crim, Ann. Rev. Phys. Chem. **35**, 657 (1984); in *Advances in Gas-Phase Photochemistry and Kinetics: Molecular Photodissociation Dynamics*, edited by M. N. R. Ashfold and J. E. Baggot (Royal Society of Chemistry, London, 1987), Chap. 6, p. 177.
[2] K. V. Reddy, R. G. Bray and M. J. Berry, *Adv. Laser. Chem., 48*, edited by A. H. Zewail (Springer, Berlin, 1978).
[3] T. Uzer, Phys. Rep. (preprint).
[4] P. R. Stannard and W. M. Gelbart, J. Phys. Chem. **85**, 3592 (1981).
[5] I. Oref and B. S. Rabinovitch, Acc. Chem. Res. **12**, 166 (1979); J. D. Rynbrandt and B. S. Rabinovitch, J. Chem. Phys. **54**, 2275 (1971); J. Phys. Chem. **75**, 2164 (1971); A. B. Trenwith and B. S. Rabinovitch, J. Phys. Chem. **86**, 3447 (1982); A. B. Trenwith, D. A. Oswald, B. S. Rabinovitch, and M. C. Flowers, J. Phys. Chem. **91**, 4398 (1987).
[6] J. S. Hutchinson, W. P. Reinhardt, and J. T. Hynes, J. Chem. Phys. **79**, 4247 (1983); J. S. Hutchinson, J. T. Hynes, and W. P. Reinhardt, Chem. Phys. Lett. **108**, 353 (1984); J. S. Hutchinson, E. L. Sibert III, and J. T. Hynes, J. Chem. Phys. **81**, 1314 (1984).
[7] T. Uzer and J. T. Hynes, Chem. Phys. Lett. **113**, 483 (1985).
[8] T. A. Holme and J. S. Hutchinson, J. Chem. Phys. **83**, 2860 (1985).
[9] R. S. Smith, R. B. Shirts, and C. W. Patterson, J. Chem. Phys. **86**, 4452 (1987); R. S. Smith and R. B. Shirts, J. Chem. Phys. **89**, 2948 (1988).
[10] B. A. Waite, J. Phys. Chem. **88**, 5076 (1984).
[11] J. S. Hutchinson, J. Phys. Chem. **91**, 4495 (1987); R. P. Muller, J. S. Hutchinson, and T. A. Holme, J. Chem. Phys. **90**, 4582 (1989).
[12] B. G. Sumpter and D. L. Thompson, J. Chem. Phys. **82**, 4557 (1985); J. Chem. Phys. **86**, 2805 (1987); Chem. Phys. Lett. **153**, 243 (1988).
[13] T. Uzer, J. T. Hynes, and W. P. Reinhardt, J. Chem. Phys. **85**, 5791 (1986).
[14] B. G. Sumpter, C. C. Martens, and G. S. Ezra, J. Phys. Chem. **92**, 7193 (1988); C. Getino, B. G. Sumpter, J. Santamaria, and G. S. Ezra, J. Phys. Chem. **93**, 3877 (1989).
[15] C. S. Sloane and W. L. Hase, J. Chem. Phys. **66**, 1523 (1977).
[16] T. A. Holme and R. D. Levine, J. Chem. Phys. **89**, 3379 (1988); Chem. Phys. Lett. **150**, 393 (1988).
[17] P. Hofmann, R. B. Gerber, M. A. Ratner, L. C. Baylor, and E. Weitz, J. Chem. Phys. **88**, 7434 (1988).
[18] L. G. Spears, Jr. and J. S. Hutchinson, J. Chem. Phys. **88**, 240 (1988); J. Chem. Phys. **88**, 250.
[19] S. Kato, J. Chem. Phys. **83**, 1085 (1985).
[20] K. T. Marshall and J. S. Hutchinson, J. Phys. Chem. **91**, 3219 (1987).
[21] A. Amrein, H. Hollenstein, M. Quack, R. Zenobi, J. Segall, and R. N. Zare, J. Chem. Phys. **90**, 3944 (1989).
[22] D. A. Chernoff, J. D. Myers, and J. G. Pruett, J. Chem. Phys. **85**, 3732 (1986).
[23] P. J. Nagy and W. L. Hase, Chem. Phys. Lett. **54**, 73 (1978); Chem. Phys. Lett. **58**, 482 (1978); D-h. Lu and W. L. Hase, J. Chem. Phys. **85**, 4422 (1986); Chem. Phys. Lett. **142**, 187 (1987); J. Phys. Chem. **92**, 3217 (1988); J. Chem. Phys. **89**, 6723 (1988); J. Chem. Phys. **91**, 7490 (1989).
[24] E. L. Sibert III, W. P. Reinhardt, and J. T. Hynes, Chem. Phys. Lett. **92**, 455 (1982); J. Chem. Phys. **81**, 1115 (1984); J. Chem. Phys. **81**, 1135 (1984); E. L. Sibert III, J. S. Hutchinson, J. T.Hynes, and W. P. Reinhardt, *Ultrafast Phenomena IV*, edited by D. H. Auston and K. B. Eisenthal (Springer, New York, 1984).
[25] K. L. Bintz, D. L. Thompson, and J. W. Brady, J. Chem. Phys. **85**, 1848 (1986).
[26] K. L. Bintz and D. L. Thompson, and J. W. Brady, Chem. Phys. Lett. **131**, 398 (1986); J. Chem. Phys. **86**, 4411 (1987); Y. Guan and D. L. Thompson, J. Chem. Phys. **88**, 2355 (1988).
[27] D. L. Clarke and M. A. Collins, J. Chem. Phys. **86**, 6871 (1987); J. Chem. Phys. **87**, 5312 (1987).
[28] Y. Guan and D. L. Thompson, J. Chem. Phys. **92** (1990).
[29] B. G. Sumpter and D. L. Thompson, J. Chem. Phys. **86**, 3301 (1987).
[30] J. S. Hutchinson, J. T. Hynes, and W. P. Reinhardt, J. Phys. Chem. **90**, 3528 (1986).
[31] L. M. Raff, J. Chem. Phys. **89**, 5680 (1988).
[32] W. P. Reinhardt and C. Duneczky, J. Chem. Soc., Faraday Trans. 2, **84**, 1511 (1988).
[33] V. Lopez and R. A. Marcus, Chem. Phys. Lett. **93**, 232 (1982); S. M. Lederman, V. Lopez, V. Fairen, G. A. Voth, and R. A. Marcus, Chem. Phys. **139**, 171 (1989).
[34] K. N. Swamy and W. L. Hase, J. Chem. Phys. **82**, 123 (1985).
[35] H. W. Schranz, S. Nordholm, and B. C. Freasier, Chem. Phys. **108**, 69 (1986); Chem. Phys. **108**, 93; Chem. Phys. **108**, 105 (1986).
[36] T. Uzer and J. T. Hynes, J. Phys. Chem. **90**, 3524 (1986).
[37] The December 1, 1989 issue of Chem. Phys. is dedicated to mode selectivity in unimolecular reactions: Chem. Phys. **139**(1), 1–238 (1989).
[38] J. M. Jasinski, J. K. Frisoll, and C. B. Moore, J. Phys. Chem. **87**, 2209 (1983).
[39] B. G. Sumpter and D. L. Thompson, J. Chem. Phys. **88**, 6889 (1988).
[40] K. V. Reddy and M. J. Berry, Chem. Phys. Lett. **66**, 223 (1979).
[41] J. S. Segall and R. N. Zare, J. Chem. Phys. **89**, 5704 (1988).
[42] J. M. Jasinski, J. K. Frisoll, and C. B. Moore, J. Phys. Chem. **87**, 3826; J. Chem. Phys. **79**, 1312 (1983); Faraday, Discuss. Chem. Soc. **75**, 223 (1983).
[43] T. R. Rizzo and F. F. Crim, J. Chem. Phys. **76**, 2754 (1982); M. D. Likar, J. E. Baggott, and F. F. Crim, J. Chem. Phys. **90**, 6266 (1989).
[44] D. W. Chandler, W. E. Farneth, and R. N. Zare, J. Chem. Phys. **77**, 4447 (1982); M. Chuang, J. E. Baggott, D. W. Chandler, W. E. Farneth, and R. N. Zare, Faraday. Discuss. Chem. Soc. **75**, 301 (1983); J. H. Gutow, D. Klenerman, and R. N. Zare, J. Phys. Chem. **92**, 172 (1988).
[45] H. Gai, D. L. Thompson, and G. A. Fisk, J. Chem. Phys. **90**, 7055 (1989).
[46] T. Uzer and S. Chapman, in *Intramolecular and Nonlinear Dynamics*, edited by W. L. Hase (JAI, Boston, in press).
[47] K. V. Reddy and M. J. Berry, Chem. Phys. Lett. **52**, 111 (1977); Faraday Discuss. Chem. Soc. **67**, 188 (1979).
[48] H. H. Harris and D. L. Bunker, Chem. Phys. Lett. **11**, 433 (1971); D. L. Bunker, J. Chem. Phys. **57**, 332 (1972); D. L. Bunker and W. L. Hase, J. Chem. Phys. **59**, 4621 (1973); W. L. Hase, J. Chem. Phys. **69**, 4711 (1978).
[49] B. G. Sumpter and D. L. Thompson, J. Chem. Phys. **87**, 5809 (1987).
[50] P. A. McDonald and J. S. Shirk, J. Chem. Phys. **77**, 2355 (1982); A. E. Shirk and J. S. Shirk, Chem. Phys. Lett. **97**, 549 (1983).
[51] Y. Guan, G. C. Lynch, and D. L. Thompson, J. Chem. Phys. **87**, 6957 (1987); Y. Guan and D. L. Thompson, Chem. Phys. **139**, 147 (1989).
[52] S. H. Bauer and N. S. True, J. Phys. Chem. **84**, 2507 (1980); K. I. Lazaar and S. H. Bauer, J. Phys. Chem. **88**, 3052 (1984).
[53] A. Preiskorn and D. L. Thompson, J. Chem. Phys. **91**, 2299 (1989).
[54] L. M. Raff, J. Chem. Phys. **90**, 6313 (1989).
[55] T. Uzer, B. D. MacDonald, Y. Guan, and D. L. Thompson, Chem. Phys. Lett. **152**, 405 (1988); Y. Guan, T. Uzer, B. D. MacDonald, and D. L. Thompson, in Advances in Molecular Vibrations and Collision Dynamics, edited by J. M. Bowman and M. Ratner (in press).
[56] C. Getino, B. G. Sumpter, and J. Santamaria, Chem. Phys. (submitted).
[57] S. Ruhman, Y. Haas, J. Laukemper, M. Preuss, H. Stein, D. Feldmann, and K. H. Welge, J. Phys. Chem. **88**, 5162 (1984).
[58] W. L. Hase, R. J. Wolf, and C. S. Sloane, J. Chem. Phys. **71**, 2911 (1979); W. L. Hase, D. G. Buckowski, J. Comput. Chem. **3**, 335 (1982); W. L. Hase, D. G. Buckowski, and K. N. Swamy, J. Phys. Chem. **87**, 2754 (1983).
[59] P. Rogers, D. C. Montague, J. P. Frank, S. C. Tyler, and F. S. Rowland, Chem. Phys. Lett. **89**, 9 (1982); P. J. Rogers, J. I. Selco, and F. S. Rowland, Chem. Phys. Lett. **97**, 313 (1983).
[60] S. P. Wrigley and B. S. Rabinovitch, Chem. Phys. Lett. **98**, 386 (1983); S.

P. Wrigley, D. A. Oswald, and B. S. Rabinovitch, Chem. Phys. Lett. **104**, 521 (1984).
[61] T. Uzer and J. T. Hynes, Chem. Phys. **139**, 163 (1989).
[62] A. J. Bowles, A. Hudson, and R. A. Jackson, Chem. Phys. Lett. **5**, 552 (1979); J. Cooper, A. Hudson, and R. A. Jackson, Tetrahedron Lett. **11**, 831 (1973).
[63] A. R. Rossi and D. E. Wood, J. Am. Chem. Soc. **98**, 3452 (1976).
[64] T. K. Minton, G. M. Nathanson, and Y. T. Lee, Laser Chem. **7**, 297 (1987).
[65] I. Biddles and A. Hudson, Chem. Phys. Lett. **18**, 45 (1973).
[66] A. C. Hopkinson, M. H. Lien, and I. G. Csizmadia, Chem. Phys. Lett. **71**, 557, 1980.
[67] H. B. Schelgel and C. Sosa, J. Phys. Chem. **88**, 1141 (1984).
[68] J. L. Holmes and F. P. Lossing, J. Am. Chem. Soc. **110**, 7343 (1988).
[69] F. Bernardi and J. Fossey, J. Mol. Struct. (Theochem), **180**, 79 (1988).
[70] J. D. Myers (personal communication).
[71] J. L. Duncan, D. C. McKean, and P. D. Mallinson, J. Mol. Spectrosc. **45**, 221 (1973).
[72] C. W. Gullikson and J. R. Nielsen, J. Mol. Spectrosc. **1**, 158 (1957).
[73] L. M. Raff, J. Phys. Chem. **91**, 3266 (1987).
[74] D. Kivelson and E. B. Wilson, Jr., J. Chem. Phys. **32**, 205 (1960).
[75] J. E. Douglas, B. S. Rabinovitch, and F. S. Looney, J. Chem. Phys. **23**, 315 (1955).
[76] V. Staemmler, Theoret. Chim. Acta (Berl.) **45**, 89 (1977).
[77] M. Said, D. Maynau, J. P. Malrieu, and M. A. G. Bach, J. Am. Chem. Soc. **106**, 571 (1984).
[78] H. Ichikawa, Y. Erisawa, and A. Shigihara, Bull. Chem. Soc. Jpn. **58**, 3619 (1985).
[79] P. L. Muller-Remmers and K. Jug, Int. J. Quant. Chem. **28**, 703 (1985).
[80] For example, D. L. Bunker, Methods Comput. Phys. **10**, 287 (1971); L. M. Raff and D. L. Thompson, in *Theory of Chemical Reaction Dynamics*, edited by M. Baer (Chemical Rubber, Boca Raton, Florida 1985).
[81] P. Carsky and R. Zahradnik, J. Mol. Struct. **54**, 247 (1979).
[82] P. Pulay, G. Fogarasi, and J. E. Boggs, J. Chem. Phys. **74**, 3999 (1981); K. Fan and J. E. Boggs, J. Mol. Struct. (Theochem) **138**, 401 (1986).
[83] R. J. Wolf, D. S. Bhatia, and W. L. Hase, Chem. Phys. Lett. **132**, 493 (1986).
[84] S. Kato and K. Morokuma, J. Chem. Phys. **72**, 206 (1980).
[85] L. S. Kassel, J. Phys. Chem. **32**, 225 (1928).